bioRxiv preprint doi: https://doi.org/10.1101/2020.05.21.109371; this version posted May 25, 2020. The copyright holder for this preprint (which was not certified by peer review) is the author/funder, who has granted bioRxiv a license to display the preprint in perpetuity. It is made available under aCC-BY-NC-ND 4.0 International license.

Natural Genetic Variation in *Drosophila melanogaster* Reveals Genes Associated with *Coxiella burnetii* Infection

Authors: Rosa M. Guzman[*,#], Zachary P. Howard[*,#], Ziying Liu[*], Ryan D. Oliveira[†], Alisha T. Massa[†], Anders Omsland[§], Stephen N. White[†,‡,**], Alan G. Goodman[*,§,1]

[*]*School of Molecular Biosciences, College of Veterinary Medicine, Washington State University, Pullman WA, 99164, USA*

[†]*Department of Veterinary Microbiology and Pathology, College of Veterinary Medicine, Washington State University, Pullman WA, 99164, USA*

[‡]*USDA-ARS Animal Disease Research, Pullman WA, 99164, USA*

[§]*Paul G. Allen School for Global Animal Health, College of Veterinary Medicine, Washington State University, Pullman WA, 99164, USA*

[**]*Center for Reproductive Biology, Washington State University, Pullman WA, 99164, USA*

[#]*Equal author contribution*

Running title: Genes that regulate *Coxiella in vivo*

Keywords: genome-wide association study; bacteria; pathogenesis; immunity; host response

[1]Corresponding Author
Alan G. Goodman
Washington State University
School of Molecular Biosciences
100 Dairy Rd., BLS 135
Pullman, WA 99164
alan.goodman@wsu.edu

bioRxiv preprint doi: https://doi.org/10.1101/2020.05.21.109371; this version posted May 25, 2020. The copyright holder for this preprint (which was not certified by peer review) is the author/funder, who has granted bioRxiv a license to display the preprint in perpetuity. It is made available under aCC-BY-NC-ND 4.0 International license.

ABSTRACT

The gram-negative bacterium *Coxiella burnetii* is the causative agent of Query (Q) fever in humans and coxiellosis in livestock. Association between host genetic background and *Coxiella burnetii* pathogenesis has been demonstrated both in humans and animals; however, specific genes associated with severity of infection remain unknown. We employed the *Drosophila* Genetics Reference Panel to perform a genome-wide association study and identify host genetic variants that affect *Coxiella burnetii* infection outcome. The analysis resulted in 64 genome-wide suggestive ($P < 10^{-5}$) single nucleotide polymorphisms or gene variants in 25 unique genes. We examined the role of each gene in *Coxiella burnetii* infection using flies carrying a null mutation or RNAi knockdown of each gene and monitoring survival. Of the 25 candidate genes, 15 validated using at least one method. For many, this is the first report establishing involvement of these genes or their homologs with *Coxiella burnetii* susceptibility in any system. Among the validated genes, *FER* and *tara* play roles in the JAK-STAT, JNK, and decapentaplegic/TGF-β signaling pathways that are associated with the innate immune response to *Coxiella burnetii* infection. Two other two validated genes, *CG42673* and *DIP-ε,* play roles in bacterial infection and synaptic signaling but no previous association with *Coxiella burnetii* pathogenesis. Furthermore, since the mammalian ortholog of *CG13404* (*PLGRKT*) is an important regulator of macrophage function, *CG13404* could play a role in *Coxiella burnetii* susceptibility through hemocyte regulation. These insights provide a foundation for further investigation of genetics of *Coxiella burnetii* susceptibility across a wide variety of hosts.

bioRxiv preprint doi: https://doi.org/10.1101/2020.05.21.109371; this version posted May 25, 2020. The copyright holder for this preprint (which was not certified by peer review) is the author/funder, who has granted bioRxiv a license to display the preprint in perpetuity. It is made available under aCC-BY-NC-ND 4.0 International license.

INTRODUCTION

Coxiella burnetii is the causative agent of Q fever, a zoonotic disease that poses a serious threat to both human and animal health (Maurin and Raoult, 1999). Based on morbidity, low infectious dose and the environmental stability of the organism, *C. burnetii* is classified as a Category B priority pathogen by the United States NIH and CDC (Madariaga et al., 2003). It is well known that the epidemiology of Q fever is associated with the presence of infected animals; sheep, goats, cattle, and humans primarily become infected by inhalation of contaminated aerosols (Marrie et al., 1996; McQuiston et al., 2002; Schimmer et al., 2008). Therefore, reducing bacterial load in the livestock is critical to preventing Q fever outbreaks. *C. burnetii* is endemic worldwide and sporadic outbreaks have recently been reported in the United States (Anderson et al., 2013; Dahlgren et al., 2015; Karakousis et al., 2006; Kersh et al., 2013; Sondgeroth et al., 2013). A recent large outbreak of Q Fever that originated in a goat farm in the Netherlands provides a warning of the risks associated with *C. burnetii* infection where 307 million Euros were spent in public health management efforts and agricultural interventions (Roest et al., 2011a, 2011b; Schimmer et al., 2008; van Asseldonk et al., 2013). To date, no commercial Q fever vaccine is available for humans or animals in the United States, and antibiotic therapy is the only option for treating the infection in humans. Culling infected or at-risk animals has been a strategy to contain emerging outbreaks (Roest et al., 2013, 2011b, 2012). Additionally, the lack of animal models with genetic malleability and the strict requirements for BSL3 animal facilities for work with Select Agent phase I virulent strains of *C. burnetii* make it difficult to study host-pathogen interactions *in vivo*.

The host genetic background has been shown to influence the development of *C. burnetii* infection in both humans and other animals (De Lange et al., 2014; Delaby et al., 2012; Ghigo et

bioRxiv preprint doi: https://doi.org/10.1101/2020.05.21.109371; this version posted May 25, 2020. The copyright holder for this preprint (which was not certified by peer review) is the author/funder, who has granted bioRxiv a license to display the preprint in perpetuity. It is made available under aCC-BY-NC-ND 4.0 International license.

al., 2002; Leone et al., 2004; Meghari et al., 2008; Raoult et al., 2005). Experimental studies in human and mouse cells have correlated defective monocyte/macrophage activation and migration with ineffective granuloma formation and overexpression of IL-10 observed in patients with chronic Q fever (Bewley, 2013; Delaby et al., 2012; Ka et al., 2014; Meghari et al., 2008; Mehraj et al., 2013). Two recent studies performed genotyping in human population and revealed that genetic variation in innate immune genes, such as pattern recognition receptors and *IFNG*, are associated with susceptibility to Q fever (Ammerdorffer et al., 2016; Wielders et al., 2015). Despite this importance, additional unidentified factors and specific genetic variants associated with susceptibility to the infection remain largely unknown. In addition, it remains to be elucidated how host genetic factors affect bacterial load and shedding in susceptible reservoir hosts.

Previous studies have profiled mammalian host responses to *C. burnetii* infection and show that the bacteria down-regulate the host innate immune response during acute infection and that the resolution of Q fever is associated with the re-establishment of type I interferon signaling (Faugaret et al., 2014; Ghigo et al., 2002; Gorvel et al., 2014). However, the mechanisms by which *C. burnetii* targets the host innate immune pathways and the host genes that contribute to the block in innate immune activation remain largely unknown. Directed studies in humans have revealed that single-nucleotide polymorphisms (SNPs) in innate immune receptors and signaling genes such as *TLR1*, *STAT1*, *IFNG*, and *MyD88* are associated with acute or chronic Q fever (Schoffelen et al., 2015; Wielders et al., 2015). Since these studies used a targeted approach to examine SNPs in only a set of candidate genes, we aim to undertake a global, genome-wide analysis to identify gene variants associated with *C. burnetii* infection using *Drosophila melanogaster* as the host model.

bioRxiv preprint doi: https://doi.org/10.1101/2020.05.21.109371; this version posted May 25, 2020. The copyright holder for this preprint (which was not certified by peer review) is the author/funder, who has granted bioRxiv a license to display the preprint in perpetuity. It is made available under aCC-BY-NC-ND 4.0 International license.

We recently demonstrated that adult *D. melanogaster* flies are susceptible to infection with the BSL2 NMII clone 4 strain of *C. burnetii* and that this strain is able to replicate in this host (Bastos et al., 2017). Additionally, *D. melanogaster* lacking functional copies of the gram-negative bacteria sensing immune deficiency pathway (Imd) signaling genes, *PGRP-LC* and *Relish*, displayed increased susceptibility to *C. burnetii* infection. Indeed, the *D. melanogaster* model is suitable for studying host-pathogen interactions during *C. burnetii* infection. Importantly, the recently developed *Drosophila* genetics reference panel (DGRP), a fully sequenced, inbred panel of fly lines derived from a natural population, provides an efficient platform for genotype-to-phenotype associations via a genome-wide association study (Huang et al., 2014a; Mackay et al., 2012a). The DGRP has already been used to reveal genes associated with resistance/tolerance to other bacterial pathogens (Bou Sleiman et al., 2015; Howick and Lazzaro, 2017; Wang et al., 2017).

In this study, we identified genetic variants in *D. melanogaster* that were associated with susceptibility or tolerance to *C. burnetii* infection. Specifically, we obtained a list of 64 SNPs in 25 unique genes from the different GWA performed. Our analyses revealed genes with sex-specific effects on susceptibility and tolerance that have functions associated with actin binding, transcriptional response, and regulation of G-proteins. Multiple genes within the decapentaplegic (DPP) pathway, homologous to the TGF-β pathway in mammals (Gelbart, 1989), were associated with susceptibility to infection. Rho GEFs and TGF-β have been associated with the development of the *Coxiella*-containing vacuole (CCV) and pathogenesis in humans, respectively (Aguilera et al., 2009; Benoit et al., 2008c, 2008a; Pennings et al., 2015; Salinas et al., 2015; Weber et al., 2016). Importantly, all the candidate genes identified have mammalian

bioRxiv preprint doi: https://doi.org/10.1101/2020.05.21.109371; this version posted May 25, 2020. The copyright holder for this preprint (which was not certified by peer review) is the author/funder, who has granted bioRxiv a license to display the preprint in perpetuity. It is made available under aCC-BY-NC-ND 4.0 International license.

orthologs or highly conserved functions that will allow for extrapolation of the findings here to mammalian systems.

Of the 25 candidate genes identified, 15 genes significantly affected host survival during *C. burnetii* infection in *D. melanogaster* null mutants or RNAi knockdown flies. While other DGRP studies tend to use either null mutants or RNAi knockdown flies for validation studies, we used both gene disruption methods to test how the genes affect diseases severity. We also examined the effect of candidate SNPs using regulatory element analysis (modENCODE) and found some within transcription factor binding hot spots, putative enhancers, novel splicing, branch point variation, and codon usage variation that could explain how the variants may affect host gene expression ultimately altering the ability to fight infection. We show how the DGRP can be utilized to identify host genetic variants associated with sex-specific susceptibility or tolerance to *C. burnetii* infection, and have broad cross-species applications.

bioRxiv preprint doi: https://doi.org/10.1101/2020.05.21.109371; this version posted May 25, 2020. The copyright holder for this preprint (which was not certified by peer review) is the author/funder, who has granted bioRxiv a license to display the preprint in perpetuity. It is made available under aCC-BY-NC-ND 4.0 International license.

MATERIAL AND METHODS

***Drosophila melanogaster* and *C. burnetii* stocks.** Fly stocks were obtained from the Bloomington *Drosophila* Stock Center, the Vienna *Drosophila* Resource Center, Exelixis at Harvard Medical School and the Kyoto Stock Center. Fly stocks were maintained at room temperature in standard meal agar fly food at 25°C and 65°C humidity. All fly strains used are listed in **Table S1**. *C. burnetii* Nine Mile phase II (NMII) clone 4 RSA439 was propagated in Acidified Citrate Cysteine Medium 2 as previously described (Omsland et al., 2009). *C. burnetii* stocks were quantified by measuring bacterial genome equivalent (GE) using quantitative real-time PCR (qPCR) as previously described (Coleman et al., 2004).

Fly infections and hazard ratio phenotype determination. Groups of 40 male and female adult flies (two to seven days old) from each DGRP line used in this study (**Table S2 and S3**) were injected with phosphate buffered-saline (PBS) or 10^5 genome equivalents (GE) of *C. burnetii* diluted in PBS to establish infection. For injections, flies were anesthetized with CO_2 and injected with 23 nL of bacteria or PBS using a pulled glass capillary and an automatic nanoliter injector (Drummond Scientific, Broomall, PA). Individual flies were injected at the ventrolateral surface of the fly thorax and placed into new vials. After injection, mortality was monitored daily for 30 days with the flies maintained at 25°C and 68% humidity. Survival curves were analyzed by the log-rank (Mantel-Cox) test using GraphPad Prism (GraphPad Software, Inc.) to determine a hazard ratio for males and females for each DGRP line. Any line having less than three percent mortality in the mock-infected group was not included in downstream analyses.

Genome-wide association analyses using hazard ratios. Phenotype to genotype association was performed by submitting $\log_{10}$ transformed hazard ratios to the dgrp2 webtool

bioRxiv preprint doi: https://doi.org/10.1101/2020.05.21.109371; this version posted May 25, 2020. The copyright holder for this preprint (which was not certified by peer review) is the author/funder, who has granted bioRxiv a license to display the preprint in perpetuity. It is made available under aCC-BY-NC-ND 4.0 International license.

(http://dgrp2.gnets.ncsu.edu/), which adjusts the phenotype for the effects of *Wolbachia* infection and major inversions (Huang et al., 2014b; Mackay et al., 2012b). Three separate analyses were run using male, female, and combined hazard ratios for the DGRP lines used in this study (**Table S2-S4**). R was used to create QQ plots from log-transformed hazard ratios and obtain R^2 values and genomic inflation values (λ). For male and female analyses, 193 male and 195 female log-transformed hazard ratios were submitted (**Table S2 and Table S3**, respectively). SNPs and small indel variants with a P-value (mixed effects model) below 10^{-5} were considered genome-wide suggestive candidate SNPs and further analyzed. For the combined analysis, both male and female hazard ratios were submitted for 191 DGRP lines. Candidate SNPs with P-values (mixed effects model) less than 10^{-5} for the average trait or the difference (female – male) trait were selected for further study. The DGRP genome assembly (BDGP R5/dm3) was used to identify variants in candidate genes. Human orthologs of candidate genes were identified by using the DRSC Integrative Ortholog Prediction Tool (DIOPT) and the ortholog with the highest weighted score was reported (Hu et al., 2011a). Predicted functions for each candidate gene were gathered using Flybase (FB2019_02). Regulataory annotation summaries for each SNP and indel were compiled using Flybase (FB2019_02) and modENCODE utilizing variant coordinates converted to the BDGP R6/dm6 reference assembly. Regulatory annotations were expounded by reviewing publicly available data within modENCODE tracks, all noncoding features including transcription factor binding sites, histone ChIP-seq data, chromatin domain segmentation, and small RNA-seq tracks.

Validation of candidate genes. Two replicates of forty adult flies from each null mutant and RNAi knockdown for each candidate gene were injected with PBS or *C. burnetii*, as stated previously, to empirically determine the effect of knockout or knockdown of the candidate gene

bioRxiv preprint doi: https://doi.org/10.1101/2020.05.21.109371; this version posted May 25, 2020. The copyright holder for this preprint (which was not certified by peer review) is the author/funder, who has granted bioRxiv a license to display the preprint in perpetuity. It is made available under aCC-BY-NC-ND 4.0 International license.

on severity to infection. All experiments were conducted twice independently, and the results were combined to determine hazard ratios and generate mortality graphs. RNAi knockdown was performed using straight-winged progeny from crosses between the CyO-balanced *Act5C-GAL4* driver line and the corresponding dsRNA-containing RNAi lines (**Table S1**). Sibling progeny flies carrying the CyO balancer were used as control flies. Genetic background strains for each null mutant strain were used as control flies. After injection, adult flies were maintained at 25°C and 68% humidity for 30 days and mortality was monitored daily. Hazard ratios were determined from the survival curves of two combined mortality experiments and analyzed as stated previously. In addition, we employed a strict threshold of $P < 0.01$ to determine significant change from control genotype as summarized in **Table S5-6**.

Splicing, branch point variation, and codon usage analysis. The Ensembl project (http://uswest.ensembl.org/index.html) and The Human Splicing Finder (http://www.umd.be/HSF/) were used to determine splicing and branch point variation from curated sequences to determine codon usage fraction based on frequency of amino acids per thousand.

Data availability. Strains and stocks are available upon request. Genomic sequence for the DGRP is available at http://dgrp.gnets.ncsu.edu/. Supplemental material is available at FigShare. The authors affirm that all data necessary for confirming the conclusions of the article are present within the article, figures, and tables.

bioRxiv preprint doi: https://doi.org/10.1101/2020.05.21.109371; this version posted May 25, 2020. The copyright holder for this preprint (which was not certified by peer review) is the author/funder, who has granted bioRxiv a license to display the preprint in perpetuity. It is made available under aCC-BY-NC-ND 4.0 International license.

RESULTS

Susceptibility to *C. burnetii* infection is dependent on host genetic background. Previously, we determined that flies deficient in the IMD signaling pathway genes, *PGRP-LC* and *Relish*, exhibited increased susceptibility to *C. burnetii* infection (30). We also determined that the gene *eiger* contributed to decreased tolerance to *C. burnetii* infection in flies, and *eiger* mutant flies were less susceptible to *C. burnetii* infection (Bastos et al., 2017). Therefore, we hypothesized that susceptibility to *C. burnetii* infection in *Drosophila* was associated with host genetic background, and that the broad base genetic variation in the DGRP would help identify other candidate genes that effect susceptibility to *C. burnetii* infection via GWA analysis. To determine the susceptibility of each DGRP line to *C. burnetii* infection, adult males and females of each line were mock-infected or infected with *C. burnetii*. Hazard ratios were calculated using the survival curves for male and female flies and subsequently used as input for the GWA analysis (**Figure 1**). In total, 193 and 195 hazard ratios were calculated for males and females, respectively. The survival curves revealed an approximately log normal distribution of hazard ratios ranging from -0.719 to 1.643 for male flies (0.191 to 44.01, non-log-transformed) and -0.714 to 1.200 for female flies (0.1932 to 15.85, non-log-transformed) (**Table S2 and S3, Figure S1A**), which indicates that genetic polymorphisms in the DGRP lines affect susceptibility to *C. burnetii* infection. Interestingly, male flies were more susceptible than female flies overall to *C. burnetii* infection, with a mean hazard ratio of 1.90 for male flies and 1.56 for female flies ($P = 0.0015$) (**Figure S1A**). Notably, we observed three distinct susceptibility phenotypes for both male and female flies. Most DGRP lines were susceptible or resistant to *C. burnetii* infection, characterized by increased mortality in the *C. burnetii* group or similar mortality in the *C. burnetii* and mock-infected group, respectively. However, some lines exhibited decreased

bioRxiv preprint doi: https://doi.org/10.1101/2020.05.21.109371; this version posted May 25, 2020. The copyright holder for this preprint (which was not certified by peer review) is the author/funder, who has granted bioRxiv a license to display the preprint in perpetuity. It is made available under aCC-BY-NC-ND 4.0 International license.

mortality compared to the mock-infected group. Mutualistic traits maintained through the evolution of *C. burnetii* may act synergistically with specific genotypes in the DGRP lines to yield a symbiotic phenotype.

GWA analyses of DGRP hazard ratios reveals candidate SNPs. The DGRP facilitates rapid genome-wide association analyses using a quantitative phenotype via submission of a data set to the online webtool (Mackay et al., 2012a). To determine polymorphisms in the DGRP population that affect susceptibility to *C. burnetii*, the hazard ratios were submitted for analysis. However, due to genome-wide association analyses relying on parametric tests, the hazard ratios were log transformed to yield an approximately normal distribution (Shapiro-Wilke test, $P > 0.1$) prior to submission for GWA analysis (**Figure S1A**). Additionally, it was determined that hazard ratios were significantly positively correlated between male and female flies ($P = 4.99 \times 10^{-7}$), but with an r^2 value of 0.121, which indicates a weak correlation and potential sex-dependent genotypes (**Figure S1B**). Thus, hazard ratios were submitted as separate files for male and female analyses, and a single, combined file in order to identify polymorphisms that may be sex-dependent and to increase power for polymorphisms that are sex-independent. The sex-independent analysis which we termed average analysis, results in top hit SNPs that affect both sexes while the sex-dependent analysis which we termed difference analysis, results in top hits that affect one sex but not the other. A total of 193, 195, and 191 hazard ratios were submitted for males, females, and average and difference, respectively (**Table S2-S4**).

A total of 1,893,791 polymorphisms were tested in the male analysis, and 1,897,049 polymorphisms were tested in the female analysis. The combined analysis tested a total of 1,889,141 polymorphisms. In total, the GWA analyses yielded a total of 64 associated polymorphisms, of which 59 were unique polymorphisms, below the genome-wide suggestive P-

bioRxiv preprint doi: https://doi.org/10.1101/2020.05.21.109371; this version posted May 25, 2020. The copyright holder for this preprint (which was not certified by peer review) is the author/funder, who has granted bioRxiv a license to display the preprint in perpetuity. It is made available under aCC-BY-NC-ND 4.0 International license.

value threshold of 10^{-5}, as expected for studies employing the DGRP (**Table S5**). In addition, quantile-quantile (Q-Q) plots revealed no significant inflation due to dataset distribution, and lambda values ranged from 0.993 (females) to 1.002 (difference) (**Figure S2A-D**). Lastly, P-values derived from these analyses appear to be reduced overall based on the lines from the Q-Q plots and lambda values below 1 (**Figure S2A-D**).

Of the 64 polymorphisms identified from the GWA, 14 SNPs are intergenic (21.9%), three of which are within 200 base pairs upstream of nearest gene; 39 are within introns (60.9%); eight are within exons (12.5%); one is within the 5' UTR (1.6%); and two are in antisense-coding RNA within exon/introns (3.1%) (**Table S5**). Of the eight SNPs within exons, six are silent and two are missense mutations. From the 64 top SNPs, we identified 25 unique candidate genes with available stocks for gene disruption and used the DGRP genome assembly (BDGP R5/dm3) to gather predictive functions and regulatory annotations for each gene using Flybase (FB2019_02) and modENCODE (**Table 1**). For each candidate gene we also report the human ortholog with the highest weighted score from the DRSC Integrative Ortholog Prediction Tool (DIOPT).

We analyzed the chromatin state of all 25 candidate gene variants using Flybase and modENCODE and found that 12 are in transcription factor binding sites (TFBS) (48%); nine are within regions predicted to be transcriptionally silent (36%); one is within a long noncoding RNA (4%); and three are in enhancers only (12%) (**Table 1**). The SNP within the candidate gene *loco* lies within an antisense RNA that is also an enhancer and TFBS. Candidate gene functions were derived from available information on Flybase.

Validation of candidate genes. We next tested the 25 candidate genes from the different GWA (**Table 1**) by infecting and monitoring survival during *C. burnetii* infection for 30 days in

bioRxiv preprint doi: https://doi.org/10.1101/2020.05.21.109371; this version posted May 25, 2020. The copyright holder for this preprint (which was not certified by peer review) is the author/funder, who has granted bioRxiv a license to display the preprint in perpetuity. It is made available under aCC-BY-NC-ND 4.0 International license.

flies carrying a null mutation in the candidate gene or knocked down for the candidate gene by RNAi. We defined validation of candidate genes as any line that has significantly different mortality than the mock-infected and genetic control (**Tables S6 and S7**). Specifically, we employed a strict threshold of $P < 0.01$ to determine significant change from control genotype. Of the 25 candidate genes, six validated in null mutants only (24%), five in RNAi knockdown only (20%), four in both null mutants and RNAi (16%), and 10 did not validate with either method (40%) (**Figure 3A**). Mortality of w^{1118} males and females (**Figure 3B-B'**) during *C. burnetii* infection were used as the genetic control for several null mutants, including $RhoGEF64C^{MB04730}$ (**Figure 3C**), $tara^{1}$ (**Figure 3D**), and $CG13404^{f07827b}$ (**Figure 3E**). We selected these candidate genes to represent how validation was determined based on P-value and survival trend for validating genes from different categories, i.e. null-only, RNAi-only, or both. w^{1118} females (**Figure 3B**) are not susceptible to *C. burnetii* infection ($P = 0.033$) but w^{1118} males (**Figure 3B'**) are highly susceptible ($P < 0.0001$) which corroborates our previous work (Bastos et al., 2017). The candidate gene $RhoGEF64C^{MB04730}$ was selected from male-only GWA (**Figure 3C-C'**) and we observed that survival in null mutants (**Figure 3C**) was overall tolerant ($P = 0.0014$) compared to w^{1118} males (**Figure 3B'**). In contrast, there was no significant change in survival between control and RNAi genotypes (**Figure 3C'**) (control, $P = 0.0374$; RNAi, $P = 0.0130$). Thus, $RhoGEF64C^{MB04730}$ males validated only in null mutants. The candidate gene *tara* was selected from the female-only GWA and we observed that in null mutants (**Figure 3D**) and RNAi knockdown flies (**Figure 3D'**), the absence of the gene resulted in increased mortality compared to control genotypes. Specifically, $tara^{1}$ females are susceptible to infection ($P < 0.0001$) compared to w^{1118} females (**Figure 3B**) and *tara* RNAi females (**Figure 3D'**) are also susceptible ($P = 0.0025$) compared to control ($P = 0.0123$). Thus, *tara* validated for females in

bioRxiv preprint doi: https://doi.org/10.1101/2020.05.21.109371; this version posted May 25, 2020. The copyright holder for this preprint (which was not certified by peer review) is the author/funder, who has granted bioRxiv a license to display the preprint in perpetuity. It is made available under aCC-BY-NC-ND 4.0 International license.

both null mutants and RNAi knockdown flies. The candidate gene *CG13404* ^{f07827b} was selected from female-only GWA and we observed that null mutants (**Figure 3E**) are not susceptible to infection (P = 0.2737) like w^{1118} females (**Figure 3B**). In contrast, *CG13404* RNAi females (**Figure 3E'**) are susceptible to infection (P < 0.0001) while control genotype females are not (P=0.3914). Thus, *CG13404* validated only in RNAi knockdown flies.

ENCODE analysis of validated genes. Splicing and branching of precursor mRNA and abundance of tRNA codons are known to affect gene expression (Jeacock et al., 2018; Komar, 2016; Královičová et al., 2004; Sauna and Kimchi-Sarfaty, 2011; Singh and Cooper, 2012; Wang and Burge, 2008; Will and Luhrmann, 2011; Zhou et al., 2016). Therefore, we used data available from the ENCODE project to determine regulatory annotations for the SNPs in genes that validated in host survival experiments. **Table 2** summarizes the splicing and branch point analysis in terms of percent variation from wildtype and codon usage as a fraction of frequency of amino acid (SNP) per thousand over frequency of amino acid (wildtype) per thousand. Several SNPs varied at the predicted mRNA splicing sites, branch points, or codon usage compared to wildtype sequences such as the SNPs affecting the validated genes *CG34351*, *DIP-ε*, *Pura*, *tara*, *FER*, and *IP3K2*. Changes in condon usage fraction for *shn* and *CG13404* may affect these gene variants albeit to a lesser extent. Together, we use these results to hypothesize why gene variants may or not validate using null mutants and RNAi knockdown.

bioRxiv preprint doi: https://doi.org/10.1101/2020.05.21.109371; this version posted May 25, 2020. The copyright holder for this preprint (which was not certified by peer review) is the author/funder, who has granted bioRxiv a license to display the preprint in perpetuity. It is made available under aCC-BY-NC-ND 4.0 International license.

DISCUSSION

Host genetics are known to lead to differences in human Q fever severity, and previous studies using human samples were focused on specific genes such as *IFNG, STAT1, and TLR10* (Ammerdorffer et al., 2016; Wielders et al., 2015). In this study, we performed an unbiased GWAS to uncover all possible genes that may regulate *C. burnetii* infection. Our study builds on previous literature by identifying host variants that not only affect *C. burnetii* infection outcome but can also be translated to future human studies due to conserved sequences. In addition to host variants, bioinformatic analysis of regulatory elements also reveals further possible explanations for host survival differences between genotypes. Altogether, the validated genes in this study reveal both novel connections and conserved cross-species connections like hemocytes/macrophage regulation and sex-specific susceptibility differences.

To perform the GWAS we infected *D. melanogaster* lines from the DGRP library, which have known genetic variation, with *C. burnetii* and measured host survival. We then used the hazard ratios from the survival curves as input for a genome-wide association to identify host variants affecting host survival. In the genetic screen alone, over 31,000 individual fruit flies were infected yet additional power of the DGRP screen lies on the previously genetically annotated 4,565,215 naturally occurring molecular variants, including 3,976,011 high quality single/multiple nucleotide polymorphisms (SNPs/MNPs), 125,788 polymorphic microsatellites, 169,053 polymorphic insertions and 293,363 polymorphic deletions (relative to genome reference) (Mackay and Huang, 2018). Our screen revealed 64 genome-wide suggested polymorphisms, 0.0014% of the 4,565,215 total variants.

We then narrowed the 64 SNPs to 25 unique candidate genes to test host survival during *C. burnetii* infection based on fly stocks available for gene disruption using null mutants and

bioRxiv preprint doi: https://doi.org/10.1101/2020.05.21.109371; this version posted May 25, 2020. The copyright holder for this preprint (which was not certified by peer review) is the author/funder, who has granted bioRxiv a license to display the preprint in perpetuity. It is made available under aCC-BY-NC-ND 4.0 International license.

RNAi knockdown. We validated candidate genes using two rules; 1) That mutants (null or RNAi-knockdown) would have a statistically significant difference in survival compared to mock at a threshold of $P < 0.0001$, and 2) That the survival trend would differ from control genotype. Of the 25 candidate genes tested, 15 validated using either null mutants or RNAi knockdown. We did not expect that validating genes would phenotypically behave the same between null mutants and RNAi knockdown because the loss versus decreased levels of a gene may influence pathways in differently (Boettcher and McManus, 2015; Zimmer et al., 2019). Several *D. melanogaster* GWA studies use flies in which gene expression has been silenced using RNAi knockdown flies to validate candidate genes because controls for knockdown are obtained within sibling progeny of a cross (Howick and Lazzaro, 2017; Palu et al., 2019, 2020). In contrast, null mutants must be matched to a genetic control line (Chow et al., 2013; Swarup et al., 2013). Our results showed that while four candidate genes validated using both methods, 11 other candidate genes validated using one method of gene disruption (**Figure 3A**). These results suggest the need for rigor in that multiple methods should be employed when applicable for testing host survival or validating gene candidate (Ayroles et al., 2015).

Two major connections between the validated fly genes in this study and mammalian systems is the role of immune cell regulation and sex-specific differences. The gene *CG13404*, which was identified in the female-only GWA, can explain both of these themes. Host mortality in *CG13404* RNAi-knockdown flies indicated they were significantly more susceptible to infection compared to control genotype. The human ortholog of *CG13404* is the plasminogen receptor (*PLG-R_{KT})*, which is important for macrophage polarization and efferocytosis, two key components of inflammation regulation (Vago et al., 2019). The absence of *PLG-R_{KT}* causes defective plasminogen binding and inflammatory macrophage migration in both male and female

bioRxiv preprint doi: https://doi.org/10.1101/2020.05.21.109371; this version posted May 25, 2020. The copyright holder for this preprint (which was not certified by peer review) is the author/funder, who has granted bioRxiv a license to display the preprint in perpetuity. It is made available under aCC-BY-NC-ND 4.0 International license.

354 mice pups, but only female *Plg-$R_{KT}^{-/-}$* pups die two days after birth (Miles et al., 2017). We
355 hypothesize that these sex-specific differences are conserved across species given that female
356 flies knocked down for *CG13404* were more susceptible to *C. burnetii* infection.

357 In *D. melanogaster* immunity, hemocytes are the professional phagocytic cells given
358 their ability to recognize, engulf, and destroy dying cells during development and pathogens
359 during larval and adult stages (Hoffmann, 2003; Regan et al., 2013; Yano et al., 2008).
360 Hemocytes also mediate the secretion of antimicrobial peptides (AMPs) in response to pathogen
361 infection through the Toll, JAK/STAT, and Immune deficiency (Imd) pathways (Hoffmann,
362 2003; Lemaitre and Hoffmann, 2007). Recent studies in our lab have shown that hemocytes
363 support *C. burnetii* replication and induce Imd-specific AMPs (Bastos et al., 2017; Hiroyasu et
364 al., 2018). Finally, hemocytes play important roles in melanization, encapsulation, and
365 coagulation/clotting (Vlisidou and Wood, 2015). For example, embryonic hematopoesis involves
366 migration of progenitor blood cells and cytoskeleton rearrangement that requires integrins, Rho
367 family GTPases, microtubule proteins, and actin/actin-binding proteins (Comber et al., 2013;
368 Evans et al., 2010; Huelsmann, 2006; Paladi, 2004; Stramer et al., 2010; Zanet et al., 2009).
369 While it remains undetermined how these individual processes occur during *C. burnetii*
370 infection, our genetic screen identified genes that could be involved in haemocyte regulatory
371 processes such as the *Rho guanyl-exchange factor* (*RhoGEF*) gene and two putative actin-
372 binding proteins in the uncharacterized genes *CG34417* and *CG32264*. Future mechanistic
373 studies are underway to determine the role of validated genes in the context of *C. burnetii*
374 infection and will likely reveal more cross-species immune response conservation.

375 Additional connections to mammalian pathways can be extrapolated from the genes that
376 validated in both null mutants and RNAi knockdowns, i.e. *DIP-ε, FER, tara,* and *CG42673*. The

bioRxiv preprint doi: https://doi.org/10.1101/2020.05.21.109371; this version posted May 25, 2020. The copyright holder for this preprint (which was not certified by peer review) is the author/funder, who has granted bioRxiv a license to display the preprint in perpetuity. It is made available under aCC-BY-NC-ND 4.0 International license.

human orthologs of *DIP-ε, FER, tara,* and *CG42673*, are *OPCML*, *FER*, *SERTAD1*, and *NOS1AP*, respectively, based on highest weighted gene from the DRSC Integrative Ortholog Predictive Tool (DIOPT) score (Hu et al., 2011b). In flies, *tara* encodes a transcriptional co-regulator that interacts with chromatin remodeling complexes, cell cycle proteins, and the JNK signaling pathway and plays a role in ataxin-1-induced degeneration (Afonso et al., 2015; Branco et al., 2008; Calgaro et al., 2002; Fernandez-Funez et al., 2000). The ortholog *SERTAD1* is also a transcriptional co-regulator and has been linked to molecular neural abnormalities similar to *tara* (Biswas et al., 2010; Savitz et al., 2013). Interestingly, a recent study showed that induction of *SERTAD1* is IFN-independently expressed during Nipah virus infection (Glennon et al., 2015). It is known that IFN induction is tissue-dependent during *C. burnetii* infection (Hedges et al., 2016); therefore, it is plausible that *tara* is targeted during *C. burnetii* infection. We observed that the loss of *tara* lead to significantly decreased host survival during *C. burnetii* infection and future mechanistic studies on this gene may reveal novel host-pathogen interactions.

In flies, *DIP-ε* belongs to the immunoglobulin superfamily (IgSF) of *defective proboscis extension response* (Dpr) and *Dpr-interacting proteins* (DIP), which form a complex network of cell surface receptors in synaptic specificity. We observed that both null mutants and RNAi knockdown flies exhibited increased mortality to *C. burnetii* infection compared to their respective controls. We also noted that codon frequency fraction compared to wildtype is 0.27, which suggests that the SNP change results from decreased abundance of tRNA codon availability. How *DIP-ε* affects host survival at the cellular level remains unknown but for the SNP (2L_6394872), it may be due to decreased codon availability altering proper gene expression that is ultimately important to the fly to fight infection. We hypothesize that *DIP-ε* may play a novel role during infection.

bioRxiv preprint doi: https://doi.org/10.1101/2020.05.21.109371; this version posted May 25, 2020. The copyright holder for this preprint (which was not certified by peer review) is the author/funder, who has granted bioRxiv a license to display the preprint in perpetuity. It is made available under aCC-BY-NC-ND 4.0 International license.

FER, which leads to activation of DPP and is a TGF-β homolog, has recently been shown to improve survival of *Klebsiella pneumoniae* through *STAT3* when overexpressed (Dolgachev et al., 2018; Li et al., 2019; Murray, 2006). It is known that *C. burnetii* induces expression of *STAT3* and *IL-10* during murine infection (Millar et al., 2015; Murray, 2006; Textoris et al., 2010). One of these studies showed that male mice have increased gene expression of *STAT3* and *IL-10* during infection which may account for the higher susceptibility of Q fever observed in men (Textoris et al., 2010). Our study corroborates previously observed sex-specific differences in gene expression following *C. burnetii* infection given that *FER* was a top hit in the female-only GWA. We hypothesize that the absence of *FER* in females disrupts the immune response required to control infection and leads to significantly increased host mortality.

The last of our validating genes in both null mutants and RNAi knockdown is *CG42673,* an uncharacterized gene that was a top SNP (3L_9540740) hit in the difference GWA. Another DGRP GWAS found that loss-of-function of *CG42673* in blood cells significantly impaired the cellular immune response to *Staphylococcus aureus* (Nazario-Toole, 2016). Interestingly, this study also found that *dpr10* significantly affected *S. aureus* phagosome maturation while our own top hit, *dpr6* (3L_10044744_SNP) validated in RNAi knockdown. *CG42673* may function as an enhancer like its human ortholog *NOS1AP* and is perhaps a target of *C. burnetii* pathogenesis. *NOS1AP* is known to bind neural nitric oxide synthase in the brain as well as proteins involved in the spliceosome and small nucleolar ribonucleic complexes according to mass-spectrometry protein-interaction studies (Grossmann et al., 2015; Hein et al., 2015).

Another theme of this study is the role of regulatory elements among validated genes. The eukaryotic gene expression process depends on proper splicing of precursor mRNA into mature mRNA which requires spliceosome recognition at specific RNA sequences at the exon-

bioRxiv preprint doi: https://doi.org/10.1101/2020.05.21.109371; this version posted May 25, 2020. The copyright holder for this preprint (which was not certified by peer review) is the author/funder, who has granted bioRxiv a license to display the preprint in perpetuity. It is made available under aCC-BY-NC-ND 4.0 International license.

intron boundaries (Singh and Cooper, 2012; Wang and Burge, 2008). Together with the 3' and 5' splice sites, the branch site helps bind small nuclear ribonucleic proteins for efficient exon recognition and branch point variants can result in exon skipping, aberrant splicing and altered production of transcripts that ultimately cause disease (Královičová et al., 2004; Will and Luhrmann, 2011). Similarly, the relative abundance of codons encoding each amino acid affects mRNA translation/stability and transcription ultimately determining gene expression levels (Jeacock et al., 2018; Komar, 2016; Sauna and Kimchi-Sarfaty, 2011; Zhou et al., 2016). We determined regulatory annotations for SNPs in genes that affected host survival using data available in ENCODE to reason how the mutations identified by the GWA can be affecting host survival, such as by affecting transcript abundance. We found that for several SNPs in validating genes differ in splicing, branch point variation, and codon abundance compared to wildtype sequences.

For example, the candidate gene *CG34351* was selected from female-only GWA and host mortality to *C. burnetii* infection was significantly different from genetic control in null mutants only (**Figure 3A, Table S5**). We found that the SNP (2L_4702261) within this gene differs -34.14% from wildtype branch point splicing. This large negative percentage difference suggests that the branch point site is broken. The SNP in validated gene *DIP-ε* (2L_6394872) showed a codon usage fraction of 3.72, higher than would be expected for an equal usage ratio of differing codons. We also found that the SNP (3L_7623460) within *Pura* differs 7.74% from wildtype splice variation, which indicates a new splice site creation with no destruction. The SNP (3R_12079260) within *tara* differs 64.82% from wildtype splicing which also indicates a new splice site creation with no destruction. For this *tara* SNP we interpret that the new acceptor site could end the intron at alternate site and could contribute to mortality of null mutants and RNAi

bioRxiv preprint doi: https://doi.org/10.1101/2020.05.21.109371; this version posted May 25, 2020. The copyright holder for this preprint (which was not certified by peer review) is the author/funder, who has granted bioRxiv a license to display the preprint in perpetuity. It is made available under aCC-BY-NC-ND 4.0 International license.

446 knockdown flies. The insertion (3R_5218712) within *FER* differs -92.69% from wildtype
447 splicing and has no variation in branch point splicing from wildtype. The -92.69% change in
448 splicing for this *FER* SNP indicates the site is broken but the destruction is offset by a 3 base pair
449 insertion. At the host level, *FER* null mutants and RNAi knockdowns differed from control
450 genotypes, which may be partially explained by altered splicing. The SNP (X_13210675) within
451 *IP3K2* differs -17.01% from wildtype splicing and has no variation in branch point splicing from
452 wildtype. The -17.01% splicing difference in this *IP3K2* SNP indicates the splice site is broken
453 because there is destruction with no creation.

454 At the regulatory annotation level, a silent codon change (ttA/ttG) was found in the SNP
455 for *shn* (2R_7099616) (**Table 2**). However, in total, 10 unique SNPs were located within *shn*
456 from the female-only GWA (**Table S4**), this gene validated in the null mutant but not by RNAi
457 knockdown. Specifically, the shn^{1} null mutant exhibited lower mortality during *C. burnetii*
458 infection than the $y^{1}\ w^{67c23}$ genetic control, which we defined as a tolerant phenotype (**Table S5**).
459 The human ortholog of *shn* is *HIVEP2* (HIV enhancer binding protein 2) which also encodes a
460 transcription factor that binds to NF-κB of different genes and contains a zinc finger C2H2
461 transcription factor domain (Allen and Wu, 2005). Although no published studies have linked
462 *HIVEP2* or *shn* to *C. burnetii* pathobiology, *shn* is part of the decapentaplegic (DPP) pathway,
463 analogous to the human TGF-β pathway (36). Additionally, it has been shown that *C. burnetii*
464 induces expression of TGF-β1 in during atypical macrophage maturation (Benoit et al., 2008b).
465 There were no significant changes in splicing, branch point variation, or codon usage in the *shn*
466 SNP compared to wildtype therefore we suspect this gene functions with others during *C.*
467 *burnetii* infection or within a pathway not tested here. Overall, our results show that employing
468 select bioinformatic tools allows us to browse integrative-level annotations on candidate and

bioRxiv preprint doi: https://doi.org/10.1101/2020.05.21.109371; this version posted May 25, 2020. The copyright holder for this preprint (which was not certified by peer review) is the author/funder, who has granted bioRxiv a license to display the preprint in perpetuity. It is made available under aCC-BY-NC-ND 4.0 International license.

validated host variants in this study. Taken together with the host survival of variants during *C. burnetii* infection, several hypothesis-driven questions can be posed about the immune function of the variants.

In addition to connections between validated fly genes and their mammalian orthologs, there were interesting observations between the DGRP predictive effect of top hits and validating genes. According to the GWAS data, the *RhoGEF64C* SNP (3L_4738164) causes increased susceptibility (effect = -0.1709, **Table S5**). However, we observed that survival of *RhoGEF64C*^{MB04730} null mutant males had significantly improved survival compared to control genotype (**Figure 3C**) but not in RNAi experiments (**Figure 3C'**). Therefore, an opposite survival trend in the null mutant flies would only be likely if the SNP was a gain-of-function mutation, which is difficult to test. Similarly, for the SNP (X_14160126) in gene *CG13404* (effect = 0.1213) predicts less susceptibility but we observed that RNAi knockdown females were significantly more susceptible compared to control genotype (**Figure 3E'**), while null mutants had no difference in host survival during infection (**Figure 3E**). Gene product threshold effects are one possible explanation for these complex data on host survival, and overall susceptible or tolerant phenotype during infection must be tested at the host level with subsequent functional experiments must be conducted.

Our screen using the DGRP identified several gene variants that affected host survival during *C. burnetii* infection that taken together with their known function and human ortholog information, can drive new mechanism-driven questions. Importantly, this study builds on our previously developed framework utilizing the *D. melanogaster* as an animal model to dissect the innate immune response to *C. burnetii* infection (Bastos et al., 2017; Hiroyasu et al., 2018). We observed that for candidate and validated genes, regulatory element data helps explain how the

bioRxiv preprint doi: https://doi.org/10.1101/2020.05.21.109371; this version posted May 25, 2020. The copyright holder for this preprint (which was not certified by peer review) is the author/funder, who has granted bioRxiv a license to display the preprint in perpetuity. It is made available under aCC-BY-NC-ND 4.0 International license.

492 gene variants may affect host survival. In each case, identification of alternate transcripts in
493 RNA-seq data would be supportive of the functional hypotheses suggested by our bioinformatic
494 analyses. Follow up studies will need to go beyond whole organism mutants tested here, such as
495 testing minigene mutants which allow researchers to test splicing patterns *in vitro* (Cooper, 2005;
496 Ruan et al., 2015; Stoss et al., 1999). Nevertheless, the gene variants identified here highlight
497 conserved cross-species connections and an opportunity for novel discovery about their role
498 during *C. burnetii* infection.
499

bioRxiv preprint doi: https://doi.org/10.1101/2020.05.21.109371; this version posted May 25, 2020. The copyright holder for this preprint (which was not certified by peer review) is the author/funder, who has granted bioRxiv a license to display the preprint in perpetuity. It is made available under aCC-BY-NC-ND 4.0 International license.

ACKNOWLEDGEMENTS

We thank Marcos A. Perez for critical review of this manuscript. We thank Michael D. Knight, Sarah A. Borgnes, Olivia Hayden, Marina Martin, and Emily L. Kindelberger for assistance in injecting fruit flies. We thank Codie Durfee for technical assistance. We are thankful to the Drosophila Genomics Resource Center (P40OD010949), the Bloomington Drosophila Stock Center (P40OD018537), the Vienna Drosophila Stock Center, Exelixis and TRiP at Harvard Medical School (R01GM084947) for providing reagents and fly stocks. This investigation was supported by funds from Washington State University and the National Institutes of Health Public Health Service grant R21AI128103 (to A.G.G.). R.D.O. was supported by NIH Training Grant T32AI007025. This investigation's contents are solely the responsibility of the authors and do not necessarily represent the official views of the NIH.

bioRxiv preprint doi: https://doi.org/10.1101/2020.05.21.109371; this version posted May 25, 2020. The copyright holder for this preprint (which was not certified by peer review) is the author/funder, who has granted bioRxiv a license to display the preprint in perpetuity. It is made available under aCC-BY-NC-ND 4.0 International license.

LITERATURE CITED

Afonso, D.J.S., Liu, D., Machado, D.R., Pan, H., Jepson, J.E.C., Rogulja, D., Koh, K., 2015. TARANIS Functions with Cyclin A and Cdk1 in a Novel Arousal Center to Control Sleep in Drosophila. Current Biology 25, 1717–1726. https://doi.org/10.1016/j.cub.2015.05.037

Aguilera, M., Salinas, R., Rosales, E., Carminati, S., Colombo, M.I., Beron, W., 2009. Actin Dynamics and Rho GTPases Regulate the Size and Formation of Parasitophorous Vacuoles Containing Coxiella burnetii. Infection and Immunity 77, 4609–4620. https://doi.org/10.1128/IAI.00301-09

Allen, C.E., Wu, L.-C., 2005. ZAS Zinc Finger Proteins: The Other κB-Binding Protein Family, in: Iuchi, S., Kuldell, N. (Eds.), Zinc Finger Proteins, Molecular Biology Intelligence Unit. Springer US, Boston, MA, pp. 213–220. https://doi.org/10.1007/0-387-27421-9_29

Ammerdorffer, A., Stappers, M.H., Oosting, M., Schoffelen, T., Hagenaars, J.C., Bleeker-Rovers, C.P., Wegdam-Blans, M.C., Wever, P.C., Roest, H.J., van de Vosse, E., Netea, M.G., Sprong, T., Joosten, L.A., 2016. Genetic variation in TLR10 is not associated with chronic Q fever, despite the inhibitory effect of TLR10 on Coxiella burnetii-induced cytokines in vitro. Cytokine 77, 196–202. https://doi.org/10.1016/j.cyto.2015.09.005

Anderson, A., Bijlmer, H., Fournier, P.E., Graves, S., Hartzell, J., Kersh, G.J., Limonard, G., Marrie, T.J., Massung, R.F., McQuiston, J.H., Nicholson, W.L., Paddock, C.D., Sexton, D.J., 2013. Diagnosis and management of Q fever--United States, 2013: recommendations from CDC and the Q Fever Working Group. MMWR. Recommendations and reports : Morbidity and mortality weekly report. Recommendations and reports 62, 1–30.

bioRxiv preprint doi: https://doi.org/10.1101/2020.05.21.109371; this version posted May 25, 2020. The copyright holder for this preprint (which was not certified by peer review) is the author/funder, who has granted bioRxiv a license to display the preprint in perpetuity. It is made available under aCC-BY-NC-ND 4.0 International license.

535 Ayroles, J.F., Buchanan, S.M., O'Leary, C., Skutt-Kakaria, K., Grenier, J.K., Clark, A.G., Hartl,
536 D.L., de Bivort, B.L., 2015. Behavioral idiosyncrasy reveals genetic control of
537 phenotypic variability. Proc Natl Acad Sci USA 112, 6706–6711.
538 https://doi.org/10.1073/pnas.1503830112
539 Bastos, R.G., Howard, Z.P., Hiroyasu, A., Goodman, A.G., 2017. Host and Bacterial Factors
540 Control Susceptibility of Drosophila Melanogaster to Coxiella burnetii Infection. Infect.
541 Immun. 85. https://doi.org/10.1128/IAI.00218-17
542 Benoit, M., Barbarat, B., Bernard, A., Olive, D., Mege, J.-L., 2008a. Coxiella burnetii, the agent
543 of Q fever, stimulates an atypical M2 activation program in human macrophages.
544 European Journal of Immunology 38, 1065–1070. https://doi.org/10.1002/eji.200738067
545 Benoit, M., Ghigo, E., Capo, C., Raoult, D., Mege, J.-L., 2008c. The uptake of apoptotic cells
546 drives Coxiella burnetii replication and macrophage polarization: a model for Q fever
547 endocarditis. PLoS Pathog 4, e1000066–e1000066.
548 https://doi.org/10.1371/journal.ppat.1000066
549 Bewley, K.R., 2013. Animal models of Q fever (Coxiella burnetii). Comparative medicine 63,
550 469–76.
551 Biswas, S.C., Zhang, Y., Iyirhiaro, G., Willett, R.T., Rodriguez Gonzalez, Y., Cregan, S.P.,
552 Slack, R.S., Park, D.S., Greene, L.A., 2010. Sertad1 Plays an Essential Role in
553 Developmentaland Pathological Neuron Death. Journal of Neuroscience 30, 3973–3982.
554 https://doi.org/10.1523/JNEUROSCI.6421-09.2010
555 Boettcher, M., McManus, M.T., 2015. Choosing the Right Tool for the Job: RNAi, TALEN, or
556 CRISPR. Molecular Cell 58, 575–585. https://doi.org/10.1016/j.molcel.2015.04.028

bioRxiv preprint doi: https://doi.org/10.1101/2020.05.21.109371; this version posted May 25, 2020. The copyright holder for this preprint (which was not certified by peer review) is the author/funder, who has granted bioRxiv a license to display the preprint in perpetuity. It is made available under aCC-BY-NC-ND 4.0 International license.

557 Bou Sleiman, M.S., Osman, D., Massouras, A., Hoffmann, A.A., Lemaitre, B., Deplancke, B.,
558 2015. Genetic, molecular and physiological basis of variation in Drosophila gut
559 immunocompetence. Nature communications 6, 7829.
560 https://doi.org/10.1038/ncomms8829
561 Branco, J., Al-Ramahi, I., Ukani, L., Pérez, A.M., Fernandez-Funez, P., Rincón-Limas, D.,
562 Botas, J., 2008. Comparative analysis of genetic modifiers in Drosophila points to
563 common and distinct mechanisms of pathogenesis among polyglutamine diseases.
564 Human Molecular Genetics 17, 376–390. https://doi.org/10.1093/hmg/ddm315
565 Calgaro, S., Boube, M., Cribbs, D.L., Bourbon, H.-M., 2002. The Drosophila gene taranis
566 encodes a novel trithorax group member potentially linked to the cell cycle regulatory
567 apparatus. Genetics 160, 547–560.
568 Chow, C.Y., Wolfner, M.F., Clark, A.G., 2013. Using natural variation in Drosophila to discover
569 previously unknown endoplasmic reticulum stress genes. Proceedings of the National
570 Academy of Sciences 110, 9013–9018. https://doi.org/10.1073/pnas.1307125110
571 Coleman, S.A., Fischer, E.R., Howe, D., Mead, D.J., Heinzen, R.A., 2004. Temporal Analysis of
572 Coxiella burnetii Morphological Differentiation. Journal of Bacteriology 186, 7344–
573 7352. https://doi.org/10.1128/JB.186.21.7344-7352.2004
574 Comber, K., Huelsmann, S., Evans, I., Sanchez-Sanchez, B.J., Chalmers, A., Reuter, R., Wood,
575 W., Martin-Bermudo, M.D., 2013. A dual role for the PS integrin myospheroid in
576 mediating Drosophila embryonic macrophage migration. Journal of Cell Science 126,
577 3475–3484. https://doi.org/10.1242/jcs.129700
578 Cooper, T.A., 2005. Use of minigene systems to dissect alternative splicing elements. Methods
579 37, 331–340. https://doi.org/10.1016/j.ymeth.2005.07.015

bioRxiv preprint doi: https://doi.org/10.1101/2020.05.21.109371; this version posted May 25, 2020. The copyright holder for this preprint (which was not certified by peer review) is the author/funder, who has granted bioRxiv a license to display the preprint in perpetuity. It is made available under aCC-BY-NC-ND 4.0 International license.

580 Dahlgren, F.S., McQuiston, J.H., Massung, R.F., Anderson, A.D., 2015. Q fever in the United
581 States: summary of case reports from two national surveillance systems, 2000-2012. The
582 American journal of tropical medicine and hygiene 92, 247–55.
583 https://doi.org/10.4269/ajtmh.14-0503
584 De Lange, M.M., Schimmer, B., Vellema, P., Hautvast, J.L., Schneeberger, P.M., Van
585 Duijnhoven, Y.T., 2014. Coxiella burnetii seroprevalence and risk factors in sheep
586 farmers and farm residents in The Netherlands. Epidemiology and infection 142, 1231–
587 44. https://doi.org/10.1017/s0950268813001726
588 Delaby, A., Gorvel, L., Espinosa, L., Lepolard, C., Raoult, D., Ghigo, E., Capo, C., Mege, J.L.,
589 2012. Defective monocyte dynamics in Q fever granuloma deficiency. The Journal of
590 infectious diseases 205, 1086–94. https://doi.org/10.1093/infdis/jis013
591 Dolgachev, V., Panicker, S., Balijepalli, S., McCandless, L.K., Yin, Y., Swamy, S., Suresh,
592 M.V., Delano, M.J., Hemmila, M.R., Raghavendran, K., Machado-Aranda, D., 2018.
593 Electroporation-mediated delivery of FER gene enhances innate immune response and
594 improves survival in a murine model of pneumonia. Gene Ther 25, 359–375.
595 https://doi.org/10.1038/s41434-018-0022-y
596 Evans, I.R., Hu, N., Skaer, H., Wood, W., 2010. Interdependence of macrophage migration and
597 ventral nerve cord development in Drosophila embryos. Development 137, 1625–1633.
598 https://doi.org/10.1242/dev.046797
599 Faugaret, D., Ben Amara, A., Alingrin, J., Daumas, A., Delaby, A., Lepolard, C., Raoult, D.,
600 Textoris, J., Mege, J.L., 2014. Granulomatous response to Coxiella burnetii, the agent of
601 Q fever: the lessons from gene expression analysis. Frontiers in cellular and infection
602 microbiology 4, 172. https://doi.org/10.3389/fcimb.2014.00172

bioRxiv preprint doi: https://doi.org/10.1101/2020.05.21.109371; this version posted May 25, 2020. The copyright holder for this preprint (which was not certified by peer review) is the author/funder, who has granted bioRxiv a license to display the preprint in perpetuity. It is made available under aCC-BY-NC-ND 4.0 International license.

603 Fernandez-Funez, P., Nino-Rosales, M.L., de Gouyon, B., She, W.-C., Luchak, J.M., Martinez,
604 P., Turiegano, E., Benito, J., Capovilla, M., Skinner, P.J., McCall, A., Canal, I., Orr,
605 H.T., Zoghbi, H.Y., Botas, J., 2000. Identification of genes that modify ataxin-1-induced
606 neurodegeneration. Nature 408, 101–106. https://doi.org/10.1038/35040584
607 Gelbart, W.M., 1989. The decapentaplegic gene: a TGF-beta homologue controlling pattern
608 formation in Drosophila. Development 107 Suppl, 65–74.
609 Ghigo, E., Capo, C., Tung, C.H., Raoult, D., Gorvel, J.P., Mege, J.L., 2002. Coxiella burnetii
610 survival in THP-1 monocytes involves the impairment of phagosome maturation: IFN-
611 gamma mediates its restoration and bacterial killing. Journal of immunology (Baltimore,
612 Md. : 1950) 169, 4488–95.
613 Glennon, N.B., Jabado, O., Lo, M.K., Shaw, M.L., 2015. Transcriptome Profiling of the Virus-
614 Induced Innate Immune Response in Pteropus vampyrus and Its Attenuation by Nipah
615 Virus Interferon Antagonist Functions. J. Virol. 89, 7550–7566.
616 https://doi.org/10.1128/JVI.00302-15
617 Gorvel, L., Textoris, J., Banchereau, R., Ben Amara, A., Tantibhedhyangkul, W., von Bargen,
618 K., Ka, M.B., Capo, C., Ghigo, E., Gorvel, J.P., Mege, J.L., 2014. Intracellular bacteria
619 interfere with dendritic cell functions: role of the type I interferon pathway. PloS one 9,
620 e99420. https://doi.org/10.1371/journal.pone.0099420
621 Grossmann, A., Benlasfer, N., Birth, P., Hegele, A., Wachsmuth, F., Apelt, L., Stelzl, U., 2015.
622 Phospho-tyrosine dependent protein–protein interaction network. Mol Syst Biol 11, 794.
623 https://doi.org/10.15252/msb.20145968

bioRxiv preprint doi: https://doi.org/10.1101/2020.05.21.109371; this version posted May 25, 2020. The copyright holder for this preprint (which was not certified by peer review) is the author/funder, who has granted bioRxiv a license to display the preprint in perpetuity. It is made available under aCC-BY-NC-ND 4.0 International license.

624 Hedges, J.F., Robison, A., Kimmel, E., Christensen, K., Lucas, E., Ramstead, A., Jutila, M.A.,
625 2016. Type I Interferon Counters or Promotes Coxiella burnetii Replication Dependent
626 on Tissue. Infect. Immun. 84, 1815–1825. https://doi.org/10.1128/IAI.01540-15
627 Hein, M.Y., Hubner, N.C., Poser, I., Cox, J., Nagaraj, N., Toyoda, Y., Gak, I.A., Weisswange, I.,
628 Mansfeld, J., Buchholz, F., Hyman, A.A., Mann, M., 2015. A Human Interactome in
629 Three Quantitative Dimensions Organized by Stoichiometries and Abundances. Cell 163,
630 712–723. https://doi.org/10.1016/j.cell.2015.09.053
631 Hiroyasu, A., DeWitt, D.C., Goodman, A.G., 2018. Extraction of Hemocytes from Drosophila
632 melanogaster Larvae for Microbial Infection and Analysis. JoVE 57077.
633 https://doi.org/10.3791/57077
634 Hoffmann, J.A., 2003. The immune response of Drosophila. Nature 426, 33–38.
635 https://doi.org/10.1038/nature02021
636 Hu, Y., Flockhart, I., Vinayagam, A., Bergwitz, C., Berger, B., Perrimon, N., Mohr, S.E., 2011a.
637 An integrative approach to ortholog prediction for disease-focused and other functional
638 studies. BMC bioinformatics 12, 357. https://doi.org/10.1186/1471-2105-12-357
639 Huang, W., Massouras, A., Inoue, Y., Peiffer, J., Ramia, M., Tarone, A.M., Turlapati, L.,
640 Zichner, T., Zhu, D., Lyman, R.F., Magwire, M.M., Blankenburg, K., Carbone, M.A.,
641 Chang, K., Ellis, L.L., Fernandez, S., Han, Y., Highnam, G., Hjelmen, C.E., Jack, J.R.,
642 Javaid, M., Jayaseelan, J., Kalra, D., Lee, S., Lewis, L., Munidasa, M., Ongeri, F., Patel,
643 S., Perales, L., Perez, A., Pu, L., Rollmann, S.M., Ruth, R., Saada, N., Warner, C.,
644 Williams, A., Wu, Y.Q., Yamamoto, A., Zhang, Y., Zhu, Y., Anholt, R.R., Korbel, J.O.,
645 Mittelman, D., Muzny, D.M., Gibbs, R.A., Barbadilla, A., Johnston, J.S., Stone, E.A.,
646 Richards, S., Deplancke, B., Mackay, T.F., 2014a. Natural variation in genome

bioRxiv preprint doi: https://doi.org/10.1101/2020.05.21.109371; this version posted May 25, 2020. The copyright holder for this preprint (which was not certified by peer review) is the author/funder, who has granted bioRxiv a license to display the preprint in perpetuity. It is made available under aCC-BY-NC-ND 4.0 International license.

architecture among 205 Drosophila melanogaster Genetic Reference Panel lines. Genome research 24, 1193–208. https://doi.org/10.1101/gr.171546.113

Huelsmann, S., 2006. The PDZ-GEF Dizzy regulates cell shape of migrating macrophages via Rap1 and integrins in the Drosophila embryo. Development 133, 2915–2924. https://doi.org/10.1242/dev.02449

Jeacock, L., Faria, J., Horn, D., 2018. Codon usage bias controls mRNA and protein abundance in trypanosomatids. eLife 7, e32496. https://doi.org/10.7554/eLife.32496

Ka, M.B., Gondois-Rey, F., Capo, C., Textoris, J., Million, M., Raoult, D., Olive, D., Mege, J.L., 2014. Imbalance of circulating monocyte subsets and PD-1 dysregulation in Q fever endocarditis: the role of IL-10 in PD-1 modulation. PloS one 9, e107533. https://doi.org/10.1371/journal.pone.0107533

Karakousis, P.C., Trucksis, M., Dumler, J.S., 2006. Chronic Q fever in the United States. Journal of clinical microbiology 44, 2283–7. https://doi.org/10.1128/jcm.02365-05

Kersh, G.J., Fitzpatrick, K.A., Self, J.S., Priestley, R.A., Kelly, A.J., Lash, R.R., Marsden-Haug, N., Nett, R.J., Bjork, A., Massung, R.F., Anderson, A.D., 2013. Presence and persistence of Coxiella burnetii in the environments of goat farms associated with a Q fever outbreak. Applied and environmental microbiology 79, 1697–703. https://doi.org/10.1128/aem.03472-12

Komar, A.A., 2016. The Yin and Yang of codon usage. Human Molecular Genetics 25, R77–R85. https://doi.org/10.1093/hmg/ddw207

Královičová, J., Houngninou-Molango, S., Krämer, A., Vořechovský, I., 2004. Branch site haplotypes that control alternative splicing. Human Molecular Genetics 13, 3189–3202. https://doi.org/10.1093/hmg/ddh334

bioRxiv preprint doi: https://doi.org/10.1101/2020.05.21.109371; this version posted May 25, 2020. The copyright holder for this preprint (which was not certified by peer review) is the author/funder, who has granted bioRxiv a license to display the preprint in perpetuity. It is made available under aCC-BY-NC-ND 4.0 International license.

Lemaitre, B., Hoffmann, J., 2007. The Host Defense of *Drosophila melanogaster*. Annual Review of Immunology 25, 697–743. https://doi.org/10.1146/annurev.immunol.25.022106.141615

Leone, M., Honstettre, A., Lepidi, H., Capo, C., Bayard, F., Raoult, D., Mege, J.-L., 2004. Effect of Sex on Coxiella burnetii Infection: Protective Role of 17β-Estradiol. J Infect Dis 189, 339–345. https://doi.org/10.1086/380798

Li, P., Ma, Z., Yu, Y., Hu, X., Zhou, Y., Song, H., 2019. FER promotes cell migration via regulating JNK activity. Cell Prolif 52. https://doi.org/10.1111/cpr.12656

Mackay, T.F., Richards, S., Stone, E.A., Barbadilla, A., Ayroles, J.F., Zhu, D., Casillas, S., Han, Y., Magwire, M.M., Cridland, J.M., Richardson, M.F., Anholt, R.R., Barron, M., Bess, C., Blankenburg, K.P., Carbone, M.A., Castellano, D., Chaboub, L., Duncan, L., Harris, Z., Javaid, M., Jayaseelan, J.C., Jhangiani, S.N., Jordan, K.W., Lara, F., Lawrence, F., Lee, S.L., Librado, P., Linheiro, R.S., Lyman, R.F., Mackey, A.J., Munidasa, M., Muzny, D.M., Nazareth, L., Newsham, I., Perales, L., Pu, L.L., Qu, C., Ramia, M., Reid, J.G., Rollmann, S.M., Rozas, J., Saada, N., Turlapati, L., Worley, K.C., Wu, Y.Q., Yamamoto, A., Zhu, Y., Bergman, C.M., Thornton, K.R., Mittelman, D., Gibbs, R.A., 2012a. The Drosophila melanogaster Genetic Reference Panel. Nature 482, 173–8. https://doi.org/10.1038/nature10811

Mackay, T.F.C., Huang, W., 2018. Charting the genotype-phenotype map: lessons from the *Drosophila melanogaster* Genetic Reference Panel: Charting the genotype-phenotype map. WIREs Dev Biol 7, e289. https://doi.org/10.1002/wdev.289

Madariaga, M.G., Rezai, K., Trenholme, G.M., Weinstein, R.A., 2003. Q fever: a biological weapon in your backyard. The Lancet. Infectious diseases 3, 709–21.

bioRxiv preprint doi: https://doi.org/10.1101/2020.05.21.109371; this version posted May 25, 2020. The copyright holder for this preprint (which was not certified by peer review) is the author/funder, who has granted bioRxiv a license to display the preprint in perpetuity. It is made available under aCC-BY-NC-ND 4.0 International license.

693 Marrie, T.J., Stein, A., Janigan, D., Raoult, D., 1996. Route of infection determines the clinical
694 manifestations of acute Q fever. The Journal of infectious diseases 173, 484–7.
695 Maurin, M., Raoult, D., 1999. Q fever. Clinical microbiology reviews 12, 518–53.
696 McQuiston, J.H., Childs, J.E., Thompson, H.A., 2002. Q fever. Journal of the American
697 Veterinary Medical Association 221, 796–9.
698 Meghari, S., Bechah, Y., Capo, C., Lepidi, H., Raoult, D., Murray, P.J., Mege, J.L., 2008.
699 Persistent Coxiella burnetii infection in mice overexpressing IL-10: an efficient model for
700 chronic Q fever pathogenesis. PLoS pathogens 4, e23.
701 https://doi.org/10.1371/journal.ppat.0040023
702 Mehraj, V., Textoris, J., Ben Amara, A., Ghigo, E., Raoult, D., Capo, C., Mege, J.L., 2013.
703 Monocyte responses in the context of Q fever: from a static polarized model to a kinetic
704 model of activation. The Journal of infectious diseases 208, 942–51.
705 https://doi.org/10.1093/infdis/jit266
706 Miles, L.A., Baik, N., Lighvani, S., Khaldoyanidi, S., Varki, N.M., Bai, H., Mueller, B.M.,
707 Parmer, R.J., 2017. Deficiency of plasminogen receptor, Plg-R $_{KT}$, causes defects in
708 plasminogen binding and inflammatory macrophage recruitment *in vivo*. J Thromb
709 Haemost 15, 155–162. https://doi.org/10.1111/jth.13532
710 Millar, J.A., Valdés, R., Kacharia, F.R., Landfear, S.M., Cambronne, E.D., Raghavan, R., 2015.
711 Coxiella burnetii and Leishmania mexicana residing within similar parasitophorous
712 vacuoles elicit disparate host responses. Front. Microbiol. 6.
713 https://doi.org/10.3389/fmicb.2015.00794

bioRxiv preprint doi: https://doi.org/10.1101/2020.05.21.109371; this version posted May 25, 2020. The copyright holder for this preprint (which was not certified by peer review) is the author/funder, who has granted bioRxiv a license to display the preprint in perpetuity. It is made available under aCC-BY-NC-ND 4.0 International license.

714 Murray, M.J., 2006. The Fes/Fer non-receptor tyrosine kinase cooperates with Src42A to
715 regulate dorsal closure in Drosophila. Development 133, 3063–3073.
716 https://doi.org/10.1242/dev.02467
717 Nazario-Toole, A.E., 2016. Genome Wide Association Studies of Phagocytosis and the Cellular
718 Immune Response in Drosophila melanogaster. Digital Repository at the University of
719 Maryland. https://doi.org/10.13016/M26V1H
720 Omsland, A., Cockrell, D.C., Howe, D., Fischer, E.R., Virtaneva, K., Sturdevant, D.E., Porcella,
721 S.F., Heinzen, R.A., 2009. Host cell-free growth of the Q fever bacterium Coxiella
722 burnetii. Proceedings of the National Academy of Sciences 106, 4430–4434.
723 https://doi.org/10.1073/pnas.0812074106
724 Paladi, M., 2004. Function of Rho GTPases in embryonic blood cell migration in Drosophila.
725 Journal of Cell Science 117, 6313–6326. https://doi.org/10.1242/jcs.01552
726 Palu, R.A.S., Dalton, H.M., Chow, C.Y., 2020. Decoupling of Apoptosis from Activation of the
727 ER Stress Response by the *Drosophila* Metallopeptidase *superdeath*. Genetics 214, 913–
728 925. https://doi.org/10.1534/genetics.119.303004
729 Palu, R.A.S., Ong, E., Stevens, K., Chung, S., Owings, K.G., Goodman, A.G., Chow, C.Y.,
730 2019. Natural Genetic Variation Screen in *Drosophila* Identifies Wnt Signaling,
731 Mitochondrial Metabolism, and Redox Homeostasis Genes as Modifiers of Apoptosis.
732 G3 9, 3995–4005. https://doi.org/10.1534/g3.119.400722
733 Pennings, J.L.A., Kremers, M.N.T., Hodemaekers, H.M., Hagenaars, J.C.J.P., Koning, O.H.J.,
734 Renders, N.H.M., Hermans, M.H.A., de Klerk, A., Notermans, D.W., Wever, P.C.,
735 Janssen, R., 2015. Dysregulation of serum gamma interferon levels in vascular chronic Q

bioRxiv preprint doi: https://doi.org/10.1101/2020.05.21.109371; this version posted May 25, 2020. The copyright holder for this preprint (which was not certified by peer review) is the author/funder, who has granted bioRxiv a license to display the preprint in perpetuity. It is made available under aCC-BY-NC-ND 4.0 International license.

736 Fever patients provides insights into disease pathogenesis. Clin Vaccine Immunol 22,
737 664–671. https://doi.org/10.1128/CVI.00078-15
738 Raoult, D., Marrie, T., Mege, J., 2005. Natural history and pathophysiology of Q fever. The
739 Lancet. Infectious diseases 5, 219–26. https://doi.org/10.1016/s1473-3099(05)70052-9
740 Regan, J.C., Brandão, A.S., Leitão, A.B., Mantas Dias, Â.R., Sucena, É., Jacinto, A., Zaidman-
741 Rémy, A., 2013. Steroid Hormone Signaling Is Essential to Regulate Innate Immune
742 Cells and Fight Bacterial Infection in Drosophila. PLoS Pathog 9, e1003720.
743 https://doi.org/10.1371/journal.ppat.1003720
744 Roest, H.I., Bossers, A., van Zijderveld, F.G., Rebel, J.M., 2013. Clinical microbiology of
745 Coxiella burnetii and relevant aspects for the diagnosis and control of the zoonotic
746 disease Q fever. The Veterinary quarterly 33, 148–60.
747 https://doi.org/10.1080/01652176.2013.843809
748 Roest, H.I., Ruuls, R.C., Tilburg, J.J., Nabuurs-Franssen, M.H., Klaassen, C.H., Vellema, P., van
749 den Brom, R., Dercksen, D., Wouda, W., Spierenburg, M.A., van der Spek, A.N., Buijs,
750 R., de Boer, A.G., Willemsen, P.T., van Zijderveld, F.G., 2011a. Molecular epidemiology
751 of Coxiella burnetii from ruminants in Q fever outbreak, the Netherlands. Emerging
752 infectious diseases 17, 668–75. https://doi.org/10.3201/eid1704.101562
753 Roest, H.I., Tilburg, J.J., van der Hoek, W., Vellema, P., van Zijderveld, F.G., Klaassen, C.H.,
754 Raoult, D., 2011b. The Q fever epidemic in The Netherlands: history, onset, response and
755 reflection. Epidemiology and infection 139, 1–12.
756 https://doi.org/10.1017/s0950268810002268

bioRxiv preprint doi: https://doi.org/10.1101/2020.05.21.109371; this version posted May 25, 2020. The copyright holder for this preprint (which was not certified by peer review) is the author/funder, who has granted bioRxiv a license to display the preprint in perpetuity. It is made available under aCC-BY-NC-ND 4.0 International license.

757 Roest, H.J., van Gelderen, B., Dinkla, A., Frangoulidis, D., van Zijderveld, F., Rebel, J., van
758 Keulen, L., 2012. Q fever in pregnant goats: pathogenesis and excretion of Coxiella
759 burnetii. PloS one 7, e48949. https://doi.org/10.1371/journal.pone.0048949
760 Ruan, K., Zhu, Y., Li, C., Brazill, J.M., Zhai, R.G., 2015. Alternative splicing of Drosophila
761 Nmnat functions as a switch to enhance neuroprotection under stress. Nat Commun 6,
762 10057. https://doi.org/10.1038/ncomms10057
763 Salinas, R.P., Ortiz Flores, R.M., Distel, J.S., Aguilera, M.O., Colombo, M.I., Berón, W., 2015.
764 Coxiella burnetii Phagocytosis Is Regulated by GTPases of the Rho Family and the RhoA
765 Effectors mDia1 and ROCK. PLoS One 10, e0145211–e0145211.
766 https://doi.org/10.1371/journal.pone.0145211
767 Sauna, Z.E., Kimchi-Sarfaty, C., 2011. Understanding the contribution of synonymous mutations
768 to human disease. Nat Rev Genet 12, 683–691. https://doi.org/10.1038/nrg3051
769 Savitz, J., Frank, M.B., Victor, T., Bebak, M., Marino, J.H., Bellgowan, P.S.F., McKinney, B.A.,
770 Bodurka, J., Kent Teague, T., Drevets, W.C., 2013. Inflammation and neurological
771 disease-related genes are differentially expressed in depressed patients with mood
772 disorders and correlate with morphometric and functional imaging abnormalities. Brain,
773 Behavior, and Immunity 31, 161–171. https://doi.org/10.1016/j.bbi.2012.10.007
774 Schimmer, B., Morroy, G., Dijkstra, F., Schneeberger, P.M., Weers-Pothoff, G., Timen, A.,
775 Wijkmans, C., van der Hoek, W., 2008. Large ongoing Q fever outbreak in the south of
776 The Netherlands, 2008. Euro surveillance : bulletin Europeen sur les maladies
777 transmissibles = European communicable disease bulletin 13.
778 Schoffelen, T., Ammerdorffer, A., Hagenaars, J.C., Bleeker-Rovers, C.P., Wegdam-Blans, M.C.,
779 Wever, P.C., Joosten, L.A., van der Meer, J.W., Sprong, T., Netea, M.G., van Deuren,

bioRxiv preprint doi: https://doi.org/10.1101/2020.05.21.109371; this version posted May 25, 2020. The copyright holder for this preprint (which was not certified by peer review) is the author/funder, who has granted bioRxiv a license to display the preprint in perpetuity. It is made available under aCC-BY-NC-ND 4.0 International license.

780 M., van de Vosse, E., 2015. Genetic Variation in Pattern Recognition Receptors and
781 Adaptor Proteins Associated With Development of Chronic Q Fever. The Journal of
782 infectious diseases 212, 818–29. https://doi.org/10.1093/infdis/jiv113
783 Singh, R.K., Cooper, T.A., 2012. Pre-mRNA splicing in disease and therapeutics. Trends in
784 Molecular Medicine 18, 472–482. https://doi.org/10.1016/j.molmed.2012.06.006
785 Sondgeroth, K.S., Davis, M.A., Schlee, S.L., Allen, A.J., Evermann, J.F., McElwain, T.F.,
786 Baszler, T.V., 2013. Seroprevalence of Coxiella burnetii in Washington State domestic
787 goat herds. Vector borne and zoonotic diseases (Larchmont, N.Y.) 13, 779–83.
788 https://doi.org/10.1089/vbz.2013.1331
789 Stoss, O., Stoilov, P., Hartmann, A.M., Nayler, O., Stamm, S., 1999. The in vivo minigene
790 approach to analyze tissue-specific splicing. Brain Research Protocols 4, 383–394.
791 https://doi.org/10.1016/S1385-299X(99)00043-4
792 Stramer, B., Moreira, S., Millard, T., Evans, I., Huang, C.-Y., Sabet, O., Milner, M., Dunn, G.,
793 Martin, P., Wood, W., 2010. Clasp-mediated microtubule bundling regulates persistent
794 motility and contact repulsion in Drosophila macrophages in vivo. Journal of Cell
795 Biology 189, 681–689. https://doi.org/10.1083/jcb.200912134
796 Swarup, S., Huang, W., Mackay, T.F.C., Anholt, R.R.H., 2013. Analysis of natural variation
797 reveals neurogenetic networks for Drosophila olfactory behavior. Proceedings of the
798 National Academy of Sciences 110, 1017–1022.
799 https://doi.org/10.1073/pnas.1220168110
800 Textoris, J., Ban, L.H., Capo, C., Raoult, D., Leone, M., Mege, J.-L., 2010. Sex-Related
801 Differences in Gene Expression Following Coxiella burnetii Infection in Mice: Potential

bioRxiv preprint doi: https://doi.org/10.1101/2020.05.21.109371; this version posted May 25, 2020. The copyright holder for this preprint (which was not certified by peer review) is the author/funder, who has granted bioRxiv a license to display the preprint in perpetuity. It is made available under aCC-BY-NC-ND 4.0 International license.

802 Role of Circadian Rhythm. PLoS ONE 5, e12190.
803 https://doi.org/10.1371/journal.pone.0012190
804 Vago, J.P., Sugimoto, M.A., Lima, K.M., Negreiros-Lima, G.L., Baik, N., Teixeira, M.M.,
805 Perretti, M., Parmer, R.J., Miles, L.A., Sousa, L.P., 2019. Plasminogen and the
806 Plasminogen Receptor, Plg-RKT, Regulate Macrophage Phenotypic, and Functional
807 Changes. Front. Immunol. 10, 1458. https://doi.org/10.3389/fimmu.2019.01458
808 van Asseldonk, M.A., Prins, J., Bergevoet, R.H., 2013. Economic assessment of Q fever in the
809 Netherlands. Preventive veterinary medicine 112, 27–34.
810 https://doi.org/10.1016/j.prevetmed.2013.06.002
811 Vlisidou, I., Wood, W., 2015. *Drosophila* blood cells and their role in immune responses. FEBS
812 J 282, 1368–1382. https://doi.org/10.1111/febs.13235
813 Wang, J.B., Lu, H.-L., St Leger, R.J., 2017. The genetic basis for variation in resistance to
814 infection in the Drosophila melanogaster genetic reference panel. PLoS Pathog 13,
815 e1006260–e1006260. https://doi.org/10.1371/journal.ppat.1006260
816 Wang, Z., Burge, C.B., 2008. Splicing regulation: From a parts list of regulatory elements to an
817 integrated splicing code. RNA 14, 802–813. https://doi.org/10.1261/rna.876308
818 Weber, M.M., Faris, R., van Schaik, E.J., McLachlan, J.T., Wright, W.U., Tellez, A., Roman,
819 V.A., Rowin, K., Case, E.D.R., Luo, Z.-Q., Samuel, J.E., 2016. The Type IV Secretion
820 System Effector Protein CirA Stimulates the GTPase Activity of RhoA and Is Required
821 for Virulence in a Mouse Model of Coxiella burnetii Infection. Infect Immun 84, 2524–
822 2533. https://doi.org/10.1128/IAI.01554-15
823 Wielders, C.C., Hackert, V.H., Schimmer, B., Hodemaekers, H.M., de Klerk, A., Hoebe, C.J.,
824 Schneeberger, P.M., van Duynhoven, Y.T., Janssen, R., 2015. Single nucleotide

bioRxiv preprint doi: https://doi.org/10.1101/2020.05.21.109371; this version posted May 25, 2020. The copyright holder for this preprint (which was not certified by peer review) is the author/funder, who has granted bioRxiv a license to display the preprint in perpetuity. It is made available under aCC-BY-NC-ND 4.0 International license.

825 polymorphisms in immune response genes in acute Q fever cases with differences in self-
826 reported symptoms. European journal of clinical microbiology & infectious diseases :
827 official publication of the European Society of Clinical Microbiology 34, 943–50.
828 https://doi.org/10.1007/s10096-014-2310-9
829 Will, C.L., Luhrmann, R., 2011. Spliceosome Structure and Function. Cold Spring Harbor
830 Perspectives in Biology 3, a003707–a003707.
831 https://doi.org/10.1101/cshperspect.a003707
832 Yano, T., Mita, S., Ohmori, H., Oshima, Y., Fujimoto, Y., Ueda, R., Takada, H., Goldman, W.E.,
833 Fukase, K., Silverman, N., Yoshimori, T., Kurata, S., 2008. Autophagic control of listeria
834 through intracellular innate immune recognition in drosophila. Nat Immunol 9, 908–916.
835 https://doi.org/10.1038/ni.1634
836 Zanet, J., Payre, F., Plaza, S., 2009. Fascin for cell migration in Drosophila. Fly 3, 281–282.
837 https://doi.org/10.4161/fly.10315
838 Zhou, Z., Dang, Y., Zhou, M., Li, L., Yu, C., Fu, J., Chen, S., Liu, Y., 2016. Codon usage is an
839 important determinant of gene expression levels largely through its effects on
840 transcription. Proc Natl Acad Sci USA 113, E6117–E6125.
841 https://doi.org/10.1073/pnas.1606724113
842 Zimmer, A.M., Pan, Y.K., Chandrapalan, T., Kwong, R.W.M., Perry, S.F., 2019. Loss-of-
843 function approaches in comparative physiology: is there a future for knockdown
844 experiments in the era of genome editing? J Exp Biol 222, jeb175737.
845 https://doi.org/10.1242/jeb.175737
846
847

bioRxiv preprint doi: https://doi.org/10.1101/2020.05.21.109371; this version posted May 25, 2020. The copyright holder for this preprint (which was not certified by peer review) is the author/funder, who has granted bioRxiv a license to display the preprint in perpetuity. It is made available under aCC-BY-NC-ND 4.0 International license.

FIGURE LEGENDS

Figure 1. Experimental design schematic. Groups of 40 males and females per DGRP line were injected with PBS or *C. burnetii* at 10^5 bacteria/fly and host survival monitored for 30 days to obtain hazard ratios. The hazard ratios of all DGRP lines were log-transformed and used as input for a GWAS.

Figure 2. Genome-wide association analyses with hazard ratios reveal candidate genes. Manhattan plots for A) male, B) female, C) average, and D) difference GWA analyses using mixed effect P-values for all four traits from dgrp2 webtool. Highlighted SNPs with P-values below 10^{-5} are labeled with associated candidate genes.

Figure 3. Fifteen GWAS candidate genes are validated using survival rate as a metric. (A) Venn diagram summarizes the genes that validate in null mutant flies, RNAi knockdown flies, or both. A gene is validated if the P value for its survival curve (mock versus infected) changes between the control and experimental line. P value threshold were not significant (n.s.), $P < 0.01$, and $p < 0.0001$. Colors indicate the type of GWAS analysis from which the gene came. (B-B') Survival curves of control w^{1118} (B) females and (B') males following mock or *C. burnetii* infection. (C-E) Survival curves of $RhoGEF64C^{KG02832}$ (C) or control and *RhoGEF64C* RNAi males (C'), $tara^{1}$ (D) or control and *tara* RNAi females (D'), or $CG13404^{f07827a}$ (E) or *CG13404* RNAi females (E') following mock or *C. burnetii* infection. Each survival curve represents two independent experiments of at least 40 flies that were combined for a final survival curve, Statistical significance (Log-rank test) from the mock-infected group is indicated.

bioRxiv preprint doi: https://doi.org/10.1101/2020.05.21.109371; this version posted May 25, 2020. The copyright holder for this preprint (which was not certified by peer review) is the author/funder, who has granted bioRxiv a license to display the preprint in perpetuity. It is made available under aCC-BY-NC-ND 4.0 International license.

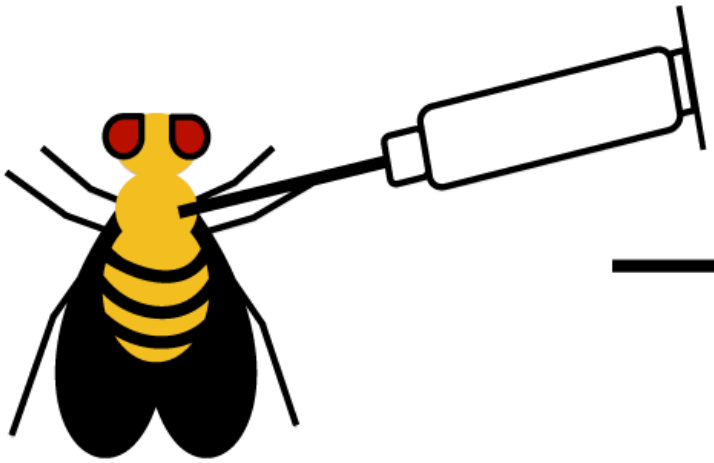

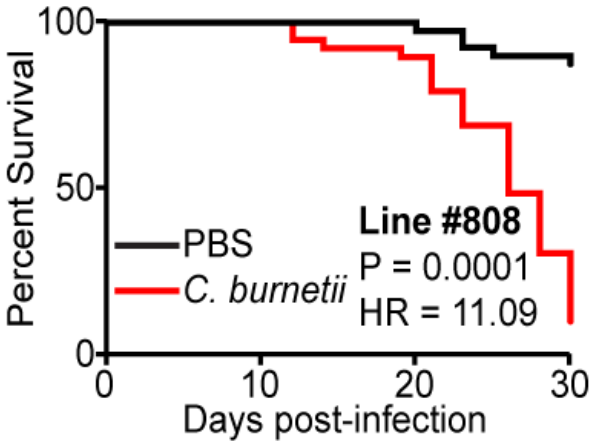

1. Infect DGRP lines with *C. burnetii* NMII

2. Record survival for 30 days and calculate hazard ratios for all lines

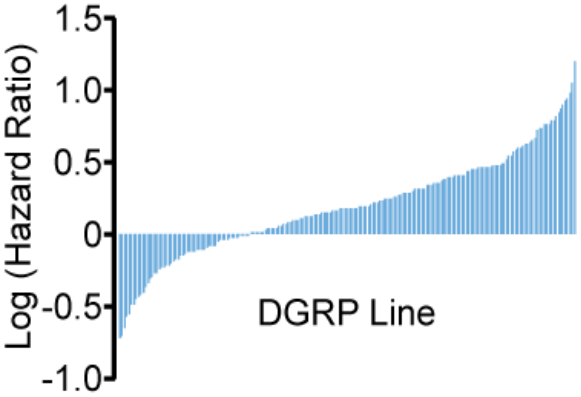

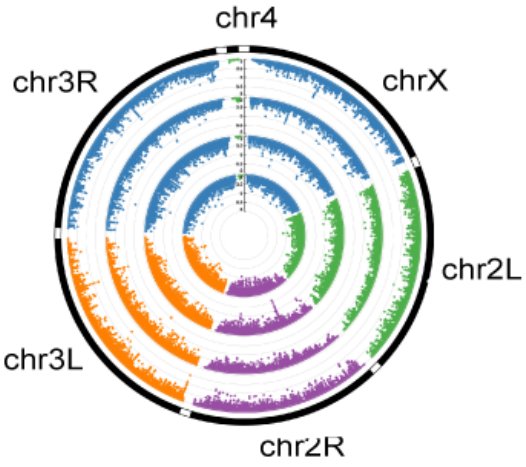

3. Submit hazard ratios to DGRP pipeline

4. Determine candidate genes using a GWAS

bioRxiv preprint doi: https://doi.org/10.1101/2020.05.21.109371; this version posted May 25, 2020. The copyright holder for this preprint (which was not certified by peer review) is the author/funder, who has granted bioRxiv a license to display the preprint in perpetuity. It is made available under aCC-BY-NC-ND 4.0 International license.

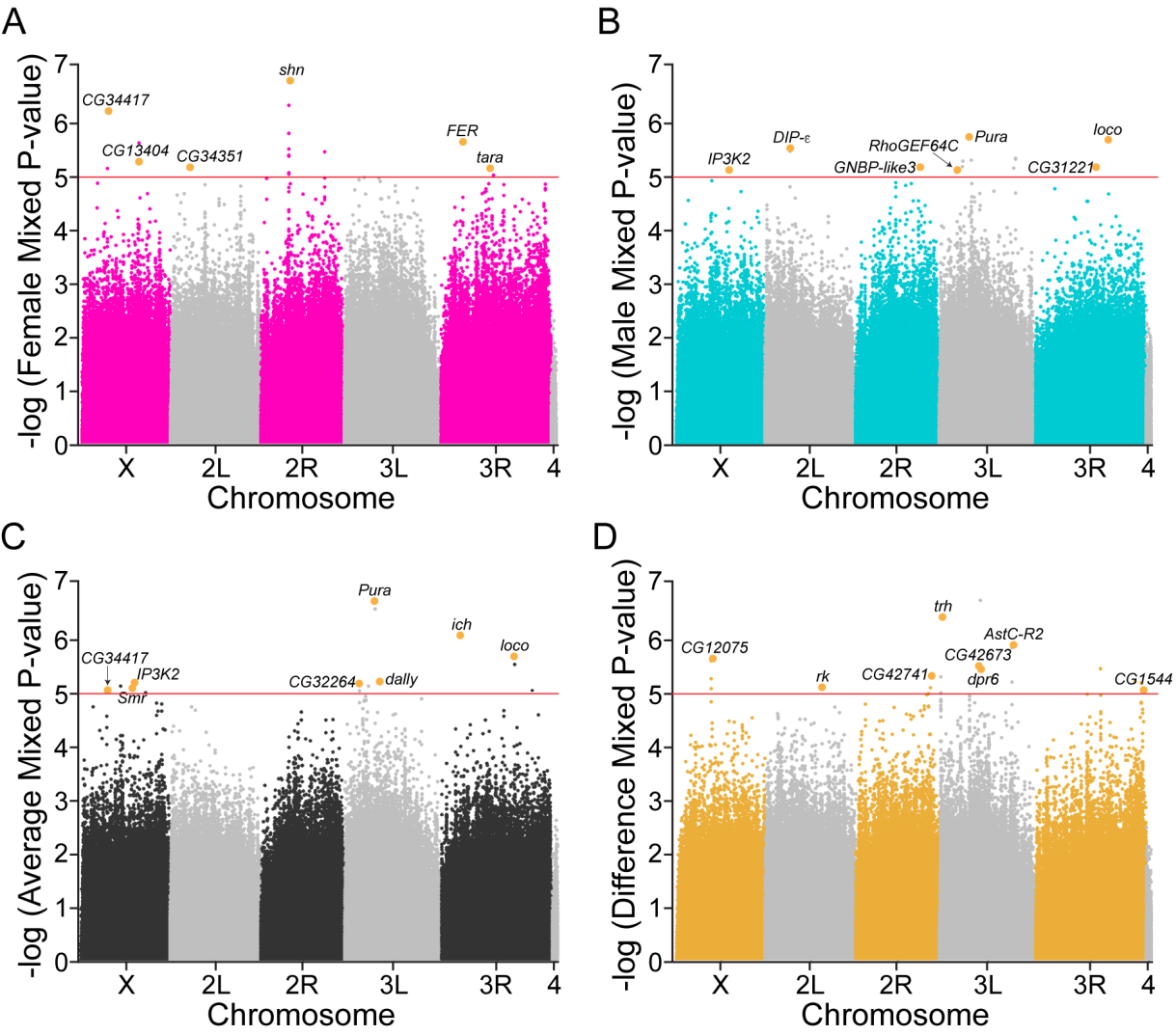

bioRxiv preprint doi: https://doi.org/10.1101/2020.05.21.109371; this version posted May 25, 2020. The copyright holder for this preprint (which was not certified by peer review) is the author/funder, who has granted bioRxiv a license to display the preprint in perpetuity. It is made available under aCC-BY-NC-ND 4.0 International license.

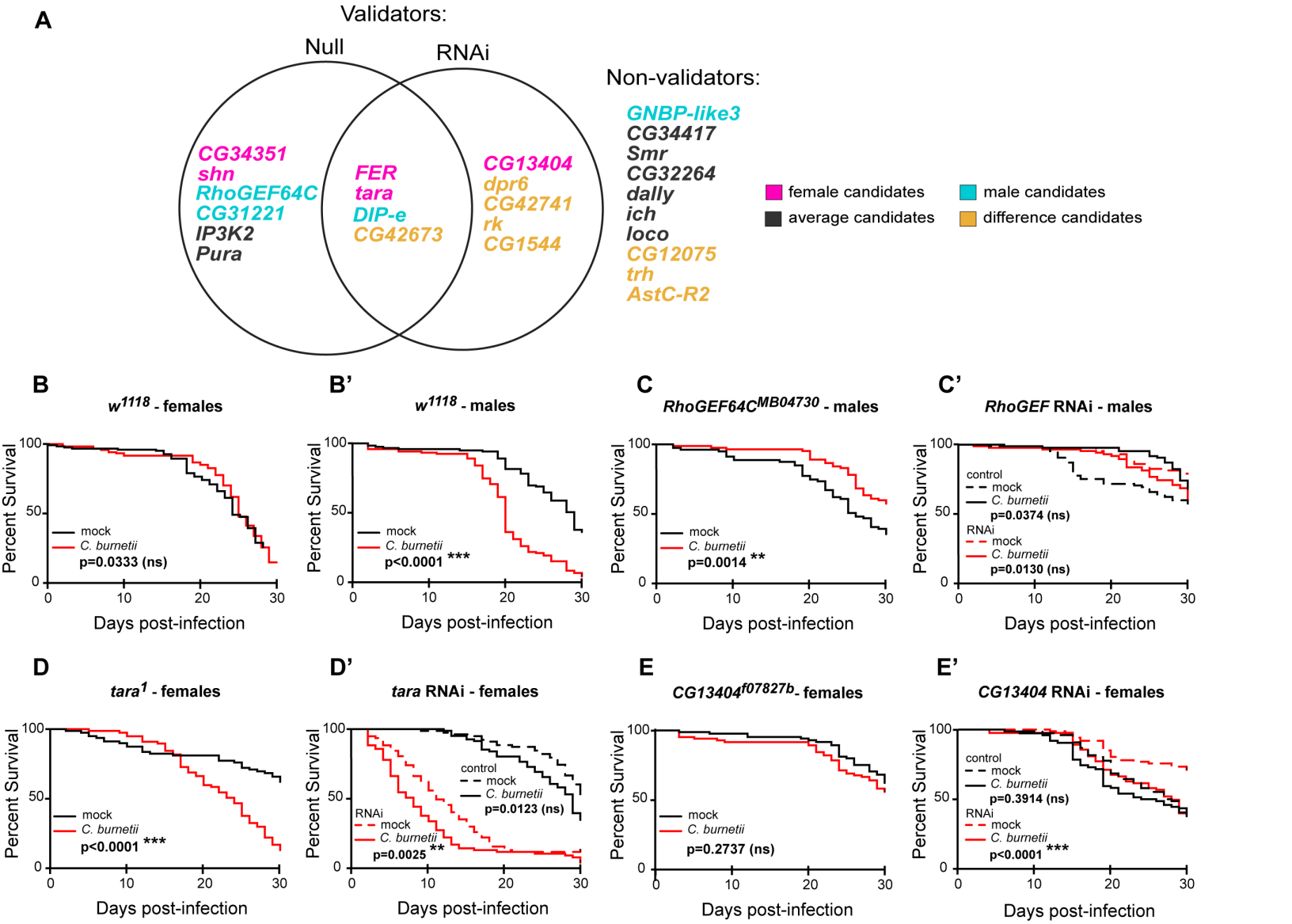

Table 1. Candidate genes associated with top SNPs from GWA analyses.

Candidate Gene	Top SNP (BDGP R5/dm3)	P-value	Analysis	Regulatory Annotations	Putative Gene Function	Human Ortholog*
CG34351	2L_4702261_SNP	$7.5x10^{-6}$	Female	Poorly annotated Euchromatin transcriptionally silent (or intergenic)	Regulation of G-proteins	RGS7BP
DIP-ε	2L_6394872_SNP	$2.9x10^{-6}$	Male	Euchromatin transcriptionally silent or dynamic	Interaction with Dprs	OPCML
rk	2L_13999491_SNP	$8.4x10^{-6}$	Difference	Transcriptionally silent	GPCR; buriscon receptor; melanization	LGR5
shn	2R_7099616_SNP	$1.9x10^{-7}$	Female	TFBS hot spot	Zinc finger C2H2 transcription factor	HIVEP2
GNBP-like3	2R_16414194_SNP	$6.1x10^{-6}$	Male	Euchromatin transcriptionally silent or dynamic	Beta 1,3-glucan recognition/binding	CRYBG1
CG42741	2R_18904195_SNP	$5.3x10^{-6}$	Difference	Transcriptionally silent	Zinc finger C2H2 transcription factor	KLF3
trh	3L_376337_SNP	$4.4x10^{-7}$	Difference	TFBS	bHLH-PAS transcription factor	NPAS1
CG32264	3L_3750617_SNP	$7.5x10^{-6}$	Average	Transcriptionally silent	Actin binding	PHACTR2
RhoGEF64C	3L_4738164_SNP	$7.4x10^{-6}$	Male	Euchromatin transcriptionally silent or dynamic	Rho guanyl-nucleotide exchange factor	ARHGEF3
Pura	3L_7623383_SNP	$2.2x10^{-7}$	Average	lncRNA	Rho guanyl-nucleotide exchange factor	PLEKHG4
dally	3L_8851042_SNP	$6.7x10^{-6}$	Average	Putative enhancer but not hot spot	Co-receptor for growth factors/morphogens	GPC5
CG42673	3L_9540740_SNP	$3.5x10^{-6}$	Difference	TFBS	Nitric-oxide synthase binding	NOS1AP
dpr6	3L_10044744_SNP	$3.8x10^{-6}$	Difference	Transcriptionally silent	Interaction with DIPs	CADM1
AstC-R2	3L_18481371_SNP	$1.4x10^{-6}$	Difference	Between two TFBS	Allatostatin receptor	SSTR2
ich	3R_4787301_SNP	$9.3x10^{-7}$	Average	TFBS hot spot	Zinc finger C2H2 transcription factor	PRDM15
FER	3R_5218712_INS	$2.7x10^{-6}$	Female	Active enhancer	Protein tyrosine kinase activity	FER
tara	3R_12079260_SNP	$7.7x10^{-6}$	Female	Active enhancer, TFBS hot spot	Transcriptional co-regulator	SERTAD1
CG31221	3R_15278653_SNP	$6.4x10^{-6}$	Male	Near TFBS	LDL receptor	LRP1B
loco	3R_18456211_SNP	$2.3x10^{-6}$	Average	Antisense RNA, enhancer, TFBS	Regulation of G-proteins	RGS12
CG1544	3R_27026419_SNP	$9.4x10^{-6}$	Difference	TFBS	Oxoglutarate dehydrogenase	DHTKD1
CG34417	X_6434578_SNP	$9.9x10^{-6}$	Average	TFBS hot spot, putative enhancer/promoter	Actin binding	SMTN
CG12075	X_8751630_SNP	$2.7x10^{-6}$	Difference	Silent chromatin state	Lipid signaling	-
Smr	X_12610055_SNP	$8.9x10^{-6}$	Average	TFBS hot spot	Chromatin binding; transcriptional regulation	NCOR1
IP3K2	X_13210675_SNP	$7.0x10^{-6}$	Average	Putative enhancer site	Calcium regulation; IP3 signaling	NET1
CG13404	X_14160126_SNP	$6.1x10^{-6}$	Female	Active enhancer, TFBS hot spot	Plasminogen receptor (KT)	PLGKRT

*human orthologs from DIOPT. Ortholog with highest weighted score reported.

Table 2. Splice, branch point, and codon usage analysis of validating genes.

Candidate gene	Top SNP (BDGP R5/dm3)	Splice Variation From Wildtype	Branch Point Variation From Wildtype	Codon change	Codon Usage Fraction (wildtype/SNP)*
CG34351	2L_4702261_SNP	No difference	-34.14%	-	-
DIP-ε	2L_6394872_SNP	N/A	N/A	Ctg/Ttg (silent)	3.72
shn	2R_7099616_SNP	N/A	N/A	ttA/ttG (silent)	1.1
Pura	3L_7623460_SNP	7.74%	No difference	-	-
tara	3R_12079260_SNP	64.82%	N/A	-	-
FER	3R_5218712_INS	-92.69%	No difference	-	-
IP3K2	X_13210675_SNP	-17.01%	No difference	-	-
CG13404	X_14160126_SNP	N/A	N/A	ctC/ctT (silent)	0.86

*Frequency of amino acid per thousand